www.czasopisma.pan.pl PAN www.journals.pan.pl

ARCHIVES of FOUNDRY ENGINEERING

ISSN (2299-2944)

10.24425/afe.2024.151314

Published quarterly as the organ of the Foundry Commission of the Polish Academy of Sciences

Modelling the Movement of Concentrate Particles in a Flash Furnace

E. Kolczyk

Łukasiewicz Research Network - Institute of Non-Ferrous Metals, Poland

Corresponding author: E-mail address: ewa.kolczyk@imn.lukasiewicz.gov.pl

Received 31.07.2024; accepted in revised form 22.10.2024; available online 24.12.2024

Abstract

Using the numerical modelling, the movement of the solid phase in the form of concentrate particles was analysed in the space of the reaction shaft and in the settler of the flash furnace. The calculations were carried out using a two-phase flow module. It was found that for all analysed concentrate particle sizes their share in the reaction shaft decreased over time. The particles moved in the form of one stream extending along the reaction shaft, accumulating on the side walls of the shaft and settler. Vortices were formed in the region of the settler tub containing particles to the upper spaces of the reaction shaft. The proportion of concentrate particles along the center of the reaction shaft after 60 s is 70 µm 1% - 3% for particles, 80 µm 0.1% - 0.7%, and for 100 µm 0,2m 0.2% - 0.7%. Along the side walls of the shaft, the shares of 70 µm particles varied between 40% and 9% over a shaft length of 5.5 m, and over 1.5 m from 12% to 10%. For 80 µm particles, the shares were 5% to 1%. The shares of 100 µm particles over a length of 1.5 m varied between 7% and 3%, and over a length of 5.5 m from 7% to 2%. Along the 70 µm reaction shaft, the concentrate particles moved the fastest at a speed of 8 m/s to 0.23 m/s. The 80 µm particles moved fastest in the range of 13 m/s to 3 m/s, and the 100 µm particles from 0.4 m/s to 2 m/s.

Keywords: Flash furnace, Movement of particles, Modelling

1. Introduction

In copper metallurgy, a flash furnace (Figure. 1) produces copper stone or metallurgical copper. The concentrate in the form of particulate particles is fed to the reaction space of the flash furnace through a concentrate burner located in the reaction shaft vault. The concentrate burner design, through which the mixture of technical air and oxygen is supplied, ensures homogenization of the concentrate and process air. During the passage of concentrate grains through the reaction shaft, they melt and oxidize flammable components. The molten reaction products accumulate in the settler below the reaction shaft, while the gaseous products flow over the bath and are directed through the gas shaft to the exhaust gas utilization system [1-4].

In recent decades, computer models used in research and development have enjoyed great interest in engineering and technology. By using CFD methods, you can optimize the process, thereby improving performance and accuracy. Modelling of phenomena that occur in a flash furnace is still too difficult and demanding for today's computer equipment. The phenomena in the reaction furnace of a flash furnace occur very quickly, which makes them difficult to observe on an industrial scale. Therefore, computer modelling is a way to study various changes in parameters affecting transport phenomena and the smelting process [5-8].

Zhu [9] modeling the behavior of particles in a flash furnace. Analyzed influence of the particle flow rate for diffrent particle size. Petteri [10] studied the phenomenon of particle settling in a flash furnace settling tank by analyzing the effect of particle coalescence, droplet collisions, and droplet property changes due to the reaction. Kumar [11] used the discrete phase model (DMP) to simulate the flow of particles with a fraction of less than 10% using the Multiple Surface Reaction in the DPM module. He

studied the effect of process air/distribution air ration, oxidant coefficient, particle size. Gao [12] optimized the particle heating process by studying the effect of convection and radiation, the high speed preheated oxygen jet, distribution of the SO_2 concentration field. Jylna [13] studied the formation of a channeling flow by using simulated flow in oil model.

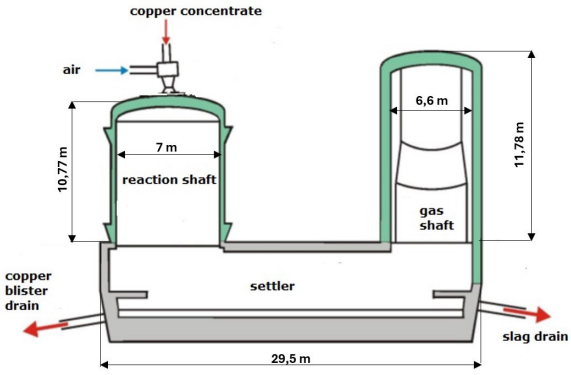

Fig. 1. Schema of flash furnace

The aim of the work was to investigate the movement of concentrate particles and their distribution depending on the particle size in the reaction shaft and part of the settling tank of the suspension furnace using numerical modelling. Characteristics of concentrate grain distribution and particle velocity distributions inside the flash furnace were developed.

2. Material and methodology

On the basis of industrial data, the average value of the technological air flow was assumed to be 38350 nm^3/h with 100 Mg/h concentrate feed. From the sieve analyzes of the supplied concentrates the following grain composition was adopted - Table 1.

Table 1.
Grain composition of concentrate

Fraction (mm)	Share (%)
undersize ≤ 0,071	65
> 0,071 ÷ ≤ 0,080	9
> 0,080 ÷ ≤ 0,160	14

Movement of concentrate particles was analyzed inside the reaction shaft and above the accepted level of the settler bath. The developed model does not take into account thermal phenomena and chemical reactions occurring in the reaction shaft and settler. It was assumed that the physical properties of the particles during staying in the reaction shaft and settler do not change. The physical properties of gas in the entire volume are constant. The concentrate particles are spherical. Gravity, buoyancy and resistance are acting on the concentrate molecule leaving the burner distributor.

Model calculations were performed in the Phoenics program in transient mode for a total time of 300 s. Results were recorded at an interval of 5 seconds.

The developed geometric model consisted of the following elements: reaction shaft, part of a settler, concentrate inlet, process air inlet and outlet. The geometric model included the internal dimensions of the reaction shaft and the settler. The model had the following dimensions: height 12 m, width 9 m, length 18 m.

The following technological properties were assumed for calculations air: density 1,189 kg/m^3, flux 38500 nm^3/h, concentrate properties density 3000 kg/m^3, feed 100 Mg/h, the share of particles of a given grain size in the concentrate feed, grain diameter 70 µm, 80 µm and 100 µm.

To analyze the movement of concentrate particles in a flash furnace, a two-phase flow model was used in the particulate-gas system. For this purpose, the IPSA (Inter Phase Slip Algorithm) module was used [14]. This module is based on solving Navier-Stokes equations for each phase separately. The equation of continuity for each phase is described by the formula in the general notation:

$$d(R\rho)/dt + div(R\rho V_i - Gr_i \, grad(R)) = \tilde{n}_{ij} \quad (1)$$

where:
R – phase participation
ρ – phase density [kg/m^3]
V_i – phase velocity vector [m/s]
Gr_i – phase diffusivity coefficient [ns/m^2]
$\tilde{n}_{ij}$ – indicator describing the mass flow velocity of phase i from phase j [$kg/(m^3s)$].
Calculations were performed for the k –ε model.

3. Results and discussion

Figures 2 - 3 show the distribution of concentrate grains with a diameter of 70 µm passing through the reaction shaft and settler after 5 s and 60 s. The concentrate particles introduced through the inlet spread in the central part of the reaction shaft creating two zones after 60 s. The first with a 3 % share extends along the center of the reaction shaft into the settler. The second zone occurs on the sides of the reaction shaft, where particles with a 30 % - 46 % share accumulate.

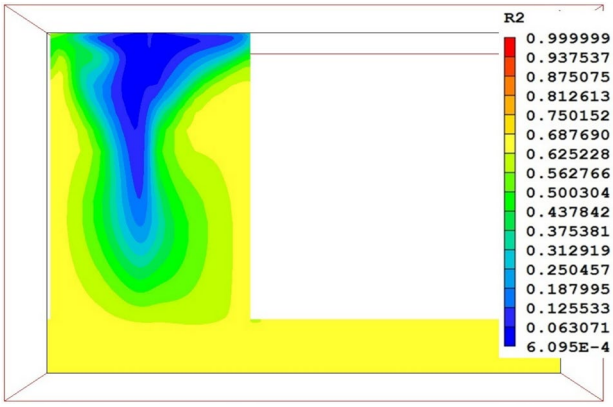

Fig. 2. Distribution of 70 µm particles during 5 s

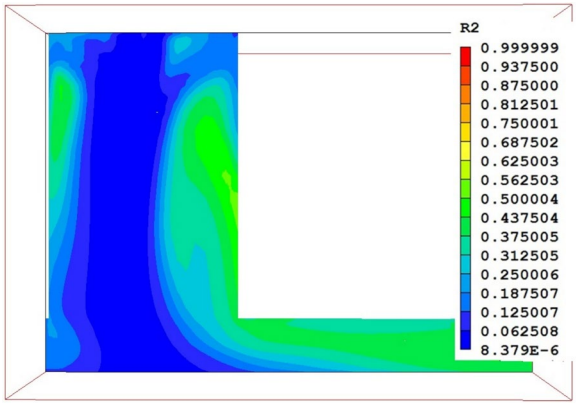

Fig. 3. Distribution of 70 µm particles after 60 s

The bar chart (Figure. 4) shows how the proportion of concentrate with a diameter of 70 µm changes during 300 s. After just 5 s the share of particles was 42 %. Over time, the proportion of concentrate particles decreased. And so after 60 s we have 3 %, and after 300 s 0.07 %.

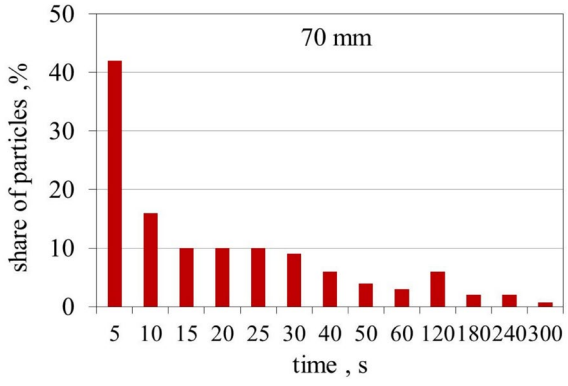

Fig. 4. Residence time 70 µm of concentrate particles in the reaction shaft

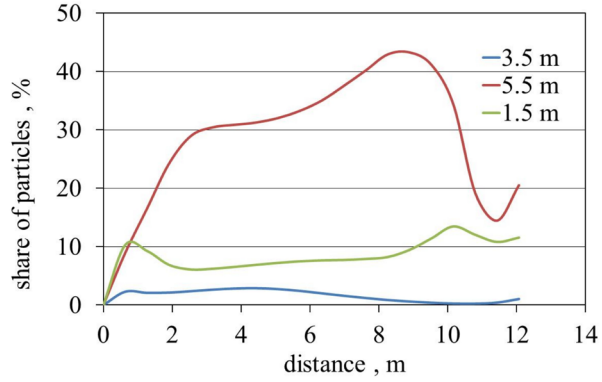

Fig. 5. Share of 70 µm concentrate particles along the reaction shaft

The change in the share of concentrate particles along the height of the reaction shaft and in the bath area just above the shaft after 60 s for three different planes is shown in Figure 5. In the plane passing through the center of the reaction shaft, which corresponds to the length of 3.5 m, the share of solid phase from the outlet - height 12 m to the bottom of the settler is at the level of 2 - 3 %. At a length of 1.5 m, the share of particles at the outlet of the shaft from 12 % decreases to 6 % at a height of 10 m to 2 m. At a height of less than 2 m, the share of the phase increased to 10 % at a height of 0.6 m. For length 5.5 m the share of particles is 43 % at a height of 8 m, and then decreases reaching 30 % at 3 m height of the shaft. The closer to the settler, the share of particles decreases reaching 0.6 m 9 %.

The concentrate particles move forming a central jet reaching up to half of the reaction shaft. In the outlet area, the particles move at speeds of 4 m/s - 17 m/s. In the remaining shaft and settler, the particles move at a speed of 1m/s to 2 m/s. The movement of the particles is directed towards the side wall of the settler, where some of them fall down, and the remaining amount moves along the settler. In the cross-section of the settler, the free fall of particles along the center of the reaction shaft is visible, followed by two-way flow of particles towards the front and rear walls of the settler, resulting in two vortices. The presence of vortices below the reaction shaft in the settler has also been found by Xia [15]. As a result, some of the concentrate particles are carried above the settler, moving up the reaction shaft (Figure. 6).

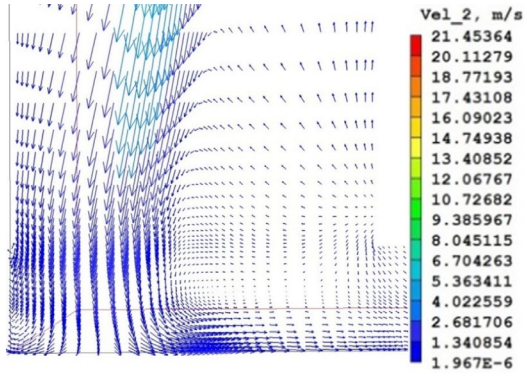

Fig. 6. Movement of 70 µm concentrate particles in the settler

The speed of the particles along the height of the reaction shaft is shown in Figure 7. At a 2.3 m shaft length, the particles move near the outlet at a speed of 0.33 m/s. As they decrease further, their speed increases, reaching 3 m/s at a height of 6.4 m, and then they slow down. On the other hand, along the 3.25 m shaft length, the particles at the outlet move at the highest speed, because 8 m/s and their speed decreases as they decrease. In the plane passing through the center of the shaft over a length of 3.5 m, as the speed decreases, the particle velocity decreases from 4 m/s to 0.12 m/s at a height of 1.3 m.

Concentrate particles with a diameter of 80 µm after 5 s diverge on the side walls of the shaft and in the settler forming a characteristic zone reaching up to half the height of the shaft, in which the share of particles is 1 % - 2 %. After 60 s in the central part of the shaft and in the settler just above the shaft, no particles are found. In the amount of 4 % - 6% they occur along the side walls of the shaft.

In the plane passing through the center of the reaction shaft for a length of 3.5 m, the share of the solid phase after 60 s from

the outlet to the settler changes at the level of 0.1 % - 0.7 %. At a length of 1.5 m, the share of particles from a 7 % share at the outlet of the shaft decreases to 3 % at a height of 1 m. Similarly at a length of 5.5 m, where from 5 % - 6 % of the share in the highest part of the reaction shaft is gradually reduced particle share.

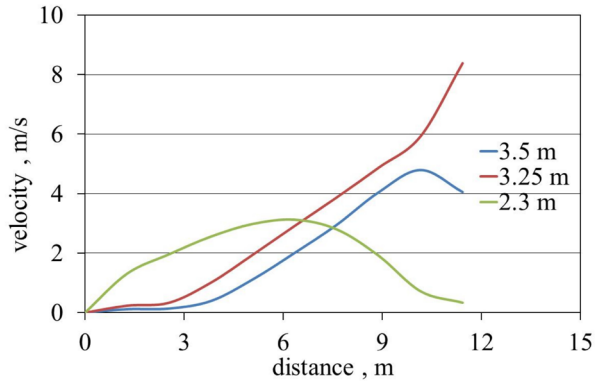

Fig. 7. Graph of particle velocity 70 μm along the reaction shaft

The solids phase of the concentrate at the outlet moves at 8 m/s - 19 m/s creating a central jet directed downwards and reaching the settler. In the reaction shaft White [7] observed the same nature of the jet with recirculation below the burner and upwards on the shaft walls. In the area of the settler, particles move along the settler and reversely return to the reaction shaft (Figure. 8). Zhou [16] reported such a reverse movement of the droplets in the settler and lifting them up to the surface of the side walls as a result of blocking by the settler walls. As a result, some of the particles begin to move upwards, and the remaining ones dissolve towards the settler. Two whirlpools are visible in the settler just above the shaft. From the side of the back of the settler and the side wall of the shaft, particles are carried up.

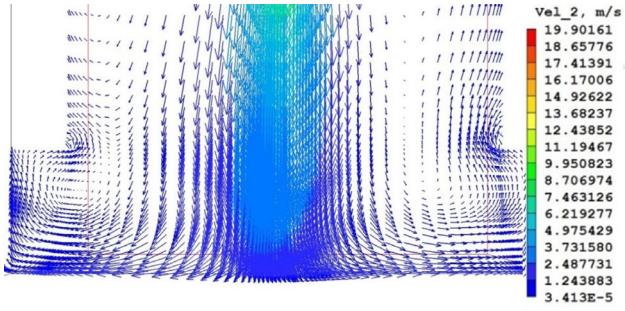

Fig. 8. Velocity distribution of 80 μm particles in cross section

At the 2.3 m and 4.5 m shaft length, the particle speed increased slightly at 1.27 m, reaching 1.4 m/s and 0.83 m/s, respectively. At a shaft length of 3.3 m, particles fly out with a maximum speed of 13 m/s and as they fall, their speed decreases reaching 1.27 m 3 m/s. In the middle of the shaft length, the particles reach a speed of 10 m/s and as they fall, they move slower at a speed of 3 m/s at a height of 1.27 m.

The distribution of concentrate particles with a diameter of 100 μm passing through the reaction shaft and settler after 5 s and 60 s is shown in Figures 9 - 10. After 5 s, a zone reaching up to half of the reaction shaft is formed in the outlet area. The share of particles in this area is negligible. After 60 s, the solid phase remains are visible only in the upper part of the shaft and on the side walls. Their share in these areas is 5 % - 10 %. The change in the share of concentrate particles during their stay in the reaction shaft is shown in Figure 11. After 5 s, the share of particles is 9 %. Their share decreases over time.

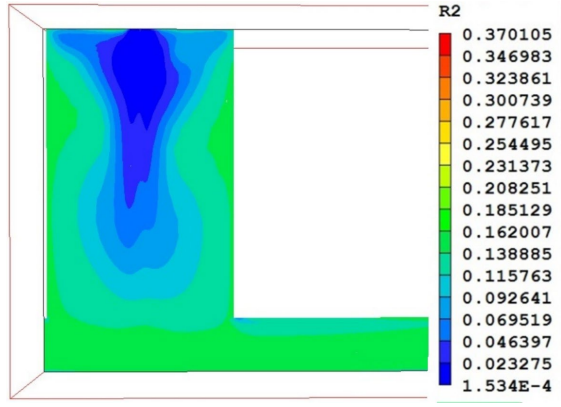

Fig. 9. Share of 100 μm particles after 5 s

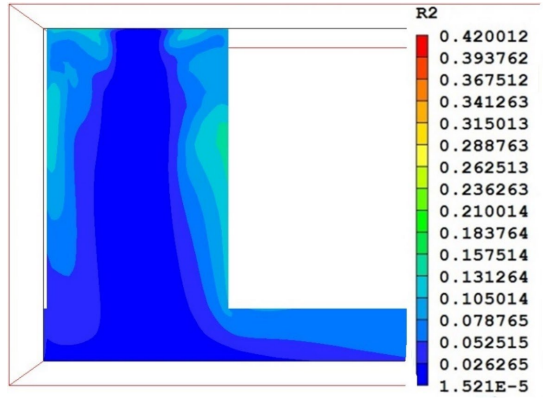

Fig. 10. Share of 100 μm particles after 60 s

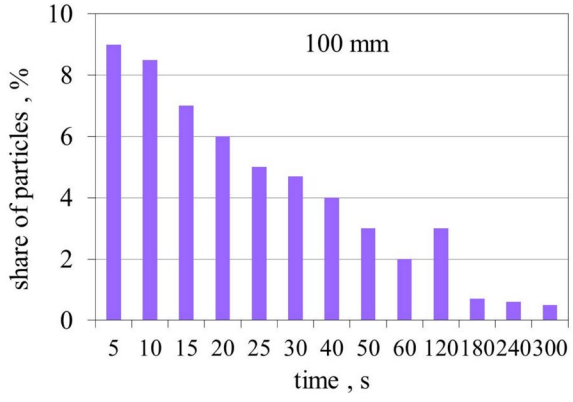

Fig. 11. Residence time of 100 μm concentrate particles in the reaction shaft

As for the change of shares along the reaction shaft, over a length of 1.5 m and 5.5 m, the share of the phase from the outlet begins to decrease. Only for a length of 5.5 m the share of particles at a shaft height of 8 m reaches a maximum share of 8 %. At the length of 3.5 m, the share of particles along the shaft is constant and amounts to 4 % (Fig. 12).

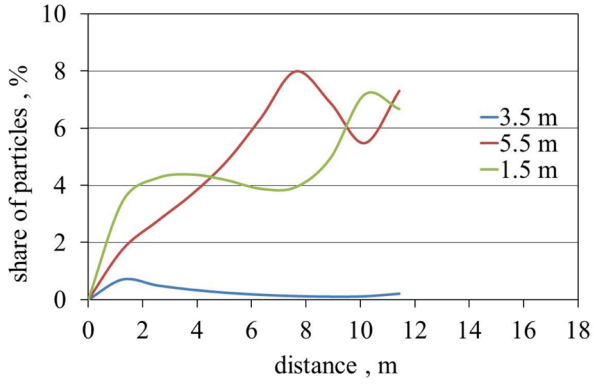

Fig. 12. Share of 100 µm particles along the shaft

In the outlet area, the concentrate particles move at speeds of 4 m/s - 18 m/s. The stream reaches the level of the settler. In the remaining shaft and settler, the particles move at a speed of 1 m/s to 2 m/s. Movement of particles in a moving stream is curved towards the side wall of the settler. In the settler, some of the particles move horizontally, while others move vortically. Reverse movement of concentrate particles reaching the top of the shaft was also found.

The velocity of particles along the reaction shaft over a length of 3.5 m is uniform (Fig. 13). The particles move from 0.53 m/s to 0.68 m/s from a height of 11 m to 1.27 m. A similar nature of the speed change along the shaft occurs at a length of 4.5 m. Only at the length of the shaft 2.5 m particles they fly out at a low speed of 0.4 m/s, then increase the speed to 3 m/s over a length of 4 m and then slow down.

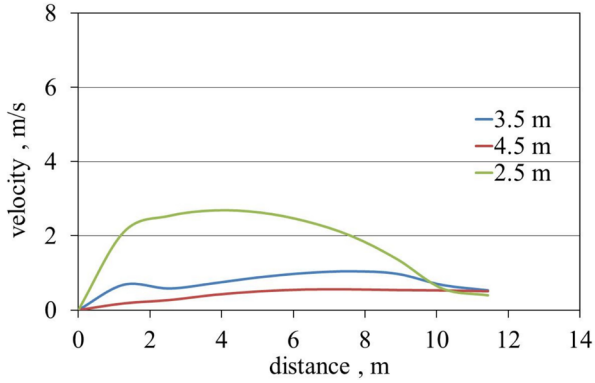

Fig. 13. Velocity graph of 100 µm particles along the shaft

4. Conclusion

For all analyzed concentrate particle sizes, the share of particles residing in the reaction shaft and in the settler decreased with time. Over time, the share of the solid phase decreases in the form of a zone propagating from the outlet of the particles from the distributor along the shaft. The particles accumulate on the side walls of the reaction shaft and in the settler.

Based on the speed distributions, it can be stated that the particles move in the form of one stream extending along the reaction shaft, diverging in the region of the settler towards the side wall and the remaining length of the settler. In the region of the front and rear walls of the settler, vortices form particles that form the upper spaces of the reaction shaft.

The share of concentrate particles along the center of the reaction shaft after 60 s is 70 µm 1 % - 3 % for particles, 80 µm 0.1 % - 0.7 %, and for 100 µm 0,2 m 0.2 % - 0.7 %. Along the side walls of the shaft, the share of 70 µm particles fluctuated in the range of 40 % - 9 % on the shaft length 5.5 m, and on 1.5 m from 12 % - 10 %. For 80 µm particles the shares were 5 % - 1 %. The share of 100 µm particles over a length of 1.5 m varied in the range of 7 % - 3 %, and over a length of 5.5 m from 7 % to 2 %.

Along the 70 µm reaction shaft, concentrate particles traveled the fastest along a 3.25 m shaft length at a speed of 8 m/s to 0.23 m/s. The 80 µm particles moved the fastest along a 3.3 m shaft length in the range of 13 m/s to 3 m/s, and 100 µm particles at a 2.5 m length from 0.4 m/s to 2 m/s.

Acknowledgements

This work was financed by the Ministry of Science and Higher Education as part of the Statutory Work of the Łukasiewicz Research Network - Institute of Non-Ferrous Metals No. 0322057008

References

[1] Piestrzyński, A. (1996). *Monograph KGHM Polska Miedź*. Lubin: Wyd. CBPM. (in Polish).

[2] Miczkowski, Z. & Czernecki, J. (2007). The influence of the size of the suspension furnace settling tank on the amount of dust discharged. *Rudy Metale*. 52(4), 172-175. UKD 66.042.8:669.046:519.6. (in Polish).

[3] Jylhä, P., Jokilaakso, A. (2019). CFD-DEM modelling of matte droplet behaviour in a flash smelting settler. In Copper International Conference, 18-21 August 2019 (pp. 1-14). Vanvcouver, Canada.

[4] Wypartowicz, J., Łędzki, A., Drożdż, P., Stachura, R. (2014) *Non-Ferrous Metallurgy. Lecture 3*. Retrieved June 3, 2014, from http://home.agh.edu.pl/~zmsz/pl/pliki/mmn/mmn_w03_miedz2. (in Polish).

[5] Jokilaakso, A., Taskinen, P. (2019). Towards a comprehensive model of the flash smelting furnace. . In

Copper International Conference, 18-21 August 2019 (pp. 1-12). Vanvcouver, Canada.
[6] Ma, Z., Turan, A., Guo, S. (2009). Practical numerical simulations of two-phase flow and heat transfer phenomena in a thermosyphon for design and development. In 9th International Conference Computational Science – ICCS, 25-27 May, (pp. 665-674). Baton Rouge, LA, USA.
[7] White, M., Haywood, D., Ranasinghe, D.J., Chen, S. (2015). The development and application of a model of copper flash smelting. In 11 International Conference on CFD in the Minerals and Process Industries, 7-8 December (pp. 1-7). Melbourne, Australia.
[8] Miettinen, E. (2017). From experimental studies to practical innovations in flash smelting. In International Proceeding Metallurgical Symposium (pp.175-186). Aalto, Finland.
[9] Zhu, Z., Zhou, P. Chem, Z. Wu, D. (2024) CFD–DEM modeling of particle segregation behavior in a simulated flash smelting furnace. *Powder Technology* 448, 120310, 1-14. DOI 10.1016/j.powtec.2024.120310
[10] Peretti, J. & Jakirakkso A. (2023). CFD–DEM modeling of particle segregation behavior in a simulated flash smelting furnace. *Heliyon.* 9, e21570, 1-16. DOI 10.1016/j.helion.2023.e21570.
[11] Kumar, N., Desai, B., Tathavadkar, V., Patel, Y., Patel, J. & Singh, A. (2023). CFD modelling of copper flash smelting furnace – reaction shaft. *Mineral Processing and Extractive Metallurgy.* 132(1), 49-61. DOI: 10.1080/25726641.2022.2160081.
[12] Gao, D., Peng, X., Song, Y. & Dai, Y. (2021). Mathematical modelling and numerical optimization of particle heating process in copper flash furnace. *Transactions of Nonferrous Metals Society of China*. 31(5), 1506-1517. DOI: 10.1016/S1003-6326(21)65594-2.
[13] Jylha, J. & Jokilzzkso, A. (2023). Settling flow details in the flash smelting furnace—a CFD-DEM simulation study. *Fluids.* 8(10), 283, 1-14. DOI 10.3390fluids8100283.
[14] CHAM Expert of CFD software and consultancy. (2015). Retrieved 2015 from http://www.cham.co.uk/phoenics/d_polis/d_enc/enc_ipsa.htm
[15] Xia, J., Ahokainen, T., Kankaanpaa, T., Jarvi, J. & Taskinen, P. (2007). Flow and heat transfer performance of slag and matte in the settler of a copper flash smelting furnace. *Steel Research International.* 78(2), 155-159. https://doi.org/10.1002/srin.200705873.
[16] Zhuo, J., Chen, Z., Zhou, P., Yu, J. & Liu, A. (2012). Numerical simulation of flow characteristics in settler of flash furnace. *Transactions of Nonferrous Metals Society of China*. 22(6), 1517-1525. DOI: 10.1016/S1003-6326(11)61350-2.